

Subnanosecond magnetization reversal of a magnetic nanoparticle driven by a chirp microwave field pulse

M. T. Islam,¹ X. S. Wang,^{1,2,*} Y. Zhang,^{1,3} and X. R. Wang^{1,3,†}

¹*Physics Department, The Hong Kong University of Science and Technology, Clear Water Bay, Kowloon, Hong Kong*

²*School of Electronic Science and Engineering and State Key Laboratory of Electronic Thin Film and Integrated Devices, University of Electronic Science and Technology of China, Chengdu, Sichuan 610054, China*

³*HKUST Shenzhen Research Institute, Shenzhen 518057, China*



(Received 16 March 2018; revised manuscript received 18 May 2018; published 13 June 2018)

We investigate the magnetization reversal of a single-domain magnetic nanoparticle driven by a linear down-chirp microwave magnetic field pulse. Numerical simulations based on the Landau-Lifshitz-Gilbert equation reveal that a down-chirp microwave pulse is solely capable of inducing subnanosecond magnetization reversal. With a certain range of initial frequency and chirp rate, the required field amplitude is much smaller than that of a constant-frequency microwave field. The fast reversal is due to the fact that the down-chirp microwave field pulse triggers stimulated microwave absorptions (emissions) by (from) the spin before (after) it crosses over the energy barrier. Applying a spin-polarized current additively to the system further reduces the microwave field amplitude. Our findings provide a way to realize low-cost and fast magnetization reversal.

DOI: [10.1103/PhysRevB.97.224412](https://doi.org/10.1103/PhysRevB.97.224412)

I. INTRODUCTION

The magnetization reversal of single-domain magnetic nanoparticles has drawn significant attention because of its application in high-density data storage [1–3] and processing [4]. Fast magnetization reversal with minimal energy cost is the ultimate demand in device applications. To achieve high thermal stability and a low error rate, high-anisotropy materials are used so that magnetic nanoparticles have a high-energy barrier [5]. It is difficult but essential to find out how to achieve the fastest magnetization reversal for high-anisotropy magnetic nanoparticles with an energy cost that is as low as possible. Over the past a few years, a number of theoretical schemes have been proposed and some of them have been verified by experiment. In the early years, a constant magnetic field was used as the driving force to reverse the magnetization [6,7], but the reversal time is too long [6] and it suffers from scalability problems because the energy consumption per unit area increases as the device feature size decreases. Since the discovery of spin transfer torque (STT) [8], the preferred way to reverse magnetization has been to deploy spin-polarized electric current [9–16], and devices based on STT magnetization reversal have been fabricated. However, a large current density is required for fast reversal so that significant Joule heat limits the device durability and reliability [17–19]. If the direction of the magnetic field or current varies with time in a designed way, the field/current amplitude or switching time can be much lower [20,21] than that of a constant field/current. But it is strenuous to generate such kinds of fields/currents in practice. A microwave magnetic field, either with or without a polarized electric current, is another

controlling knob for magnetization reversal [22–24]. A microwave of constant frequency itself can reverse magnetization through synchronization [7]. A large field amplitude is required and the reversal process is relatively slow [25–28]. Recently, there have been several studies demonstrating magnetization reversal by microwaves of time-dependent frequency [29–33]. In Refs. [29,30], magnetization reversal is induced by a combination of a static field together with a radio-frequency microwave field pulse. A dc static field is necessary and is the main reversal force, while the microwave field is only used as a reinforcement. In Ref. [30], the frequency of the microwave is always chosen to be the resonance frequency, while in Ref. [32] optimal microwave wave forms were designed. These kinds of schemes have a similar problem as the theoretical limits [20,21] that are difficult to realize. In Ref. [33], a linear down-chirp microwave field was studied, but only positive frequency f was used so that stimulated microwave emission was not allowed (microwaves with positive and negative frequencies can respectively trigger a stimulated absorption and a stimulated emission). Under such a microwave, magnetization reversal is only fast before the spin crosses its energy barrier. It takes a long time for the spin to fall into its final state because it relies on natural damping. In Ref. [34], a linear chirp microwave was studied with a theoretically estimated phase boundary of chirp rate and field amplitude. However, they did not provide a clear enough physical picture. A linearly polarized microwave was not considered, either. Thus, a fast magnetization reversal strategy with a relatively simple setup and a low-energy cost is still desired. In this paper, we show that a circularly polarized down-chirp microwave pulse (a microwave pulse whose frequency linearly decreases with time and varies from f_0 to $-f_0$) can efficiently reverse the magnetization. For a nanoparticle of high uniaxial anisotropy (coercive field $h_k \sim 0.75$ T), subnanosecond magnetization reversal can be achieved. With a proper choice of initial frequency

*Corresponding author: justicewxs@connect.ust.hk

†Corresponding author: phxwan@ust.hk

and chirp rate, the microwave field amplitude required for subnanosecond magnetization reversal is only several tens of mT, much smaller than that required for a constant-frequency microwave field. The obtained reversal time is close to the theoretical limit [20]. Also, we provide a clear physical picture for fast switching from an energy point of view. We further show that a linearly polarized down-chirp microwave field pulse is also capable of quickly reversing the magnetization. We also demonstrate that a spin-polarized current can work together with the down-chirp microwave field pulse so that both the applied current density and microwave amplitude are low enough.

II. MODEL AND METHODS

We consider a spin valve with free and fixed ferromagnetic layers and a nonmagnetic spacer in between, as shown schematically in Fig. 1(a). Both fixed and free layers are perpendicularly magnetized. The magnetization direction of the fixed layer \mathbf{p} is pinned upward, $\mathbf{p} = \hat{\mathbf{z}}$ ($\hat{\mathbf{z}}$ is the unit vector along the z direction). The magnetization of the free layer is treated as a macrospin with magnetization direction \mathbf{m} and magnitude M_s . The macrospin approximation is valid for device sizes smaller than 100 nm [35]. The Landau-Lifshitz-Gilbert (LLG) equation governs the magnetization dynamics of the free layer in the presence of spin-polarized current and a microwave magnetic field [7,20,23,28],

$$\frac{d\mathbf{m}}{dt} = -\gamma\mathbf{m} \times \mathbf{H}_{\text{eff}} - \gamma h_s \mathbf{m} \times (\mathbf{p} \times \mathbf{m}) + \alpha \mathbf{m} \times \frac{d\mathbf{m}}{dt}, \quad (1)$$

where γ is the gyromagnetic ratio, and α is the Gilbert damping constant. The total effective field \mathbf{H}_{eff} consists of the microwave magnetic field \mathbf{H}_{mw} and the anisotropy field $\mathbf{H}_K = H_K m_z \hat{\mathbf{z}}$, i.e., $\mathbf{H}_{\text{eff}} = \mathbf{H}_{\text{mw}} + \mathbf{H}_K$. h_s represents the intensity of spin transfer torque (STT) [8],

$$h_s = \frac{\hbar P j}{2e\mu_0 M_s d}, \quad (2)$$

where j , e , \hbar , P , μ_0 , and d denote the current density, electron charge, the Planck's constant, spin polarization of current, the vacuum permeability, and thickness of the free layer,

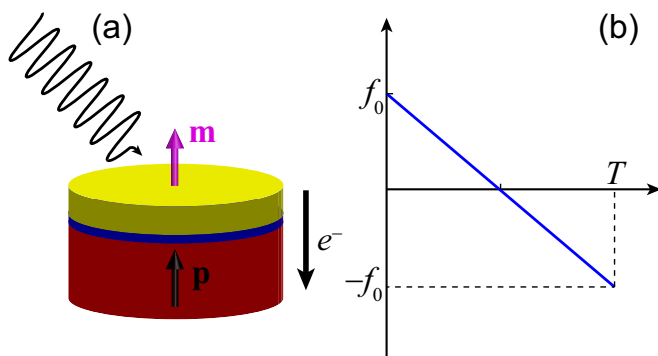


FIG. 1. (a) Schematic diagram of the system. \mathbf{m} and \mathbf{p} represent unit vectors of magnetization of free and fixed layers, respectively. A microwave field is applied onto the free layer, and an electric current flows through the spin valve. (b) The frequency of a down-chirp microwave (sweeping from $+f_0$ to $-f_0$).

respectively. In the following study, the parameters are chosen from typical experiments on microwave-driven magnetization reversal as $M_s = 10^6$ A/m, $H_k = 0.75$ T, $\gamma = 1.76 \times 10^{11}$ rad/(T s), $P = 0.6$, $\alpha = 0.01$, and $d = 2$ nm.

The microwave field \mathbf{H}_{mw} and the spin transfer torque are nonconservative forces. They do work to the macrospin. We first consider solely microwave-driven magnetization reversal. Without the STT term, the rate of energy change of the macrospin is expressed as

$$\dot{\epsilon} = -\frac{\alpha}{1+\alpha^2} |\mathbf{m} \times \mathbf{H}_{\text{eff}}|^2 - \mathbf{m} \cdot \dot{\mathbf{H}}_{\text{mw}}. \quad (3)$$

The first term is always negative because of the positive damping factor whereas the second term can be either positive or negative for a time-dependent field. In other words, the microwave field can either trigger stimulated energy absorption or emission, depending on the angle between the instantaneous magnetization direction and the time derivative of the microwave field [23].

Due to the easy-axis anisotropy, the magnetization has two stable equilibrium states, $\mathbf{m} = \pm \hat{\mathbf{z}}$, corresponding to two energy minima. The goal of magnetization reversal is to move the spin from one equilibrium state to the other. Along the way, the spin needs to cross an energy barrier at the equator ($m_z = 0$). Before \mathbf{m} reaches the equator, it gains energy from external forces. After \mathbf{m} passes the equator, it releases energy through damping or through the negative work done by external forces. For a microwave field, the ideal case for fast magnetization reversal is that the microwave always synchronizes to the magnetization motion so that $\mathbf{m} \cdot \dot{\mathbf{H}}_{\text{mw}}$ remains maximal before reaching the equator and remains minimal after passing the equator. However, this is difficult to achieve in practice. We notice that the internal effective field due to anisotropy is $\mathbf{H}_K = H_K m_z \hat{\mathbf{z}}$, which corresponds to a resonant frequency proportional to m_z . During magnetization reversal from $m_z = 1$ to $m_z = -1$, the resonant frequency decreases while the spin climbs up the potential barrier and increases while it goes down from the barrier where the spin precesses in the opposite direction. This leads us to consider a down-chirp microwave pulse, whose frequency decreases with time. If the rate of frequency change matches the magnetization precession, the microwave field roughly accommodates the magnetization precession, and it triggers stimulated microwave absorptions (emissions) by (from) magnetization before (after) the spin crosses the energy barrier so that magnetization reversal can be fast.

In order to demonstrate the feasibility of the above scenario, we apply a circularly polarized down-chirp microwave pulse on the system and numerically solve the LLG equation using the MUMAX3 package [36]. The microwave field takes the form

$$\mathbf{H}_{\text{mw}} = H_{\text{mw}} [\cos \phi(t) \hat{\mathbf{x}} + \sin \phi(t) \hat{\mathbf{y}}], \quad (4)$$

where H_{mw} is the amplitude of the microwave field and $\phi(t)$ is the phase. We consider a linear chirp whose instantaneous frequency $f(t) \equiv \frac{1}{2\pi} \frac{d\phi}{dt}$ is linearly decreasing with time at a constant rate η (in units of s^{-2}) as shown in Fig. 1(b),

$$f(t) = f_0 - \eta t, \quad \phi(t) = 2\pi \left(f_0 t - \frac{\eta}{2} t^2 \right), \quad (5)$$

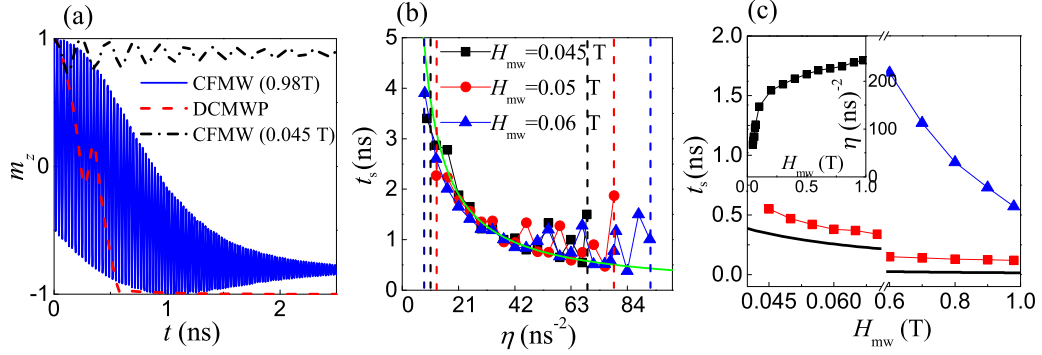


FIG. 2. (a) The time evolution of m_z driven by different sources: red dashed line for down-chirp microwave pulse (DCMWP) of $f_0 = 21$ GHz, $H_{mw} = 0.045$ T, and $\eta = 67.2$ ns⁻²; blue solid line for constant-frequency microwave (CFMW) of amplitude 0.98 T and frequency 21 GHz; black dash-dotted line for CFMW of amplitude 0.045 T and frequency 21 GHz. (b) The dependence of switching times t_s on the chirp rate η for different microwave field amplitudes H_{mw} . The vertical dashed lines are lower and upper limits of η for magnetization switching. (c) Comparison of magnetization reversal times for different strategies. The horizontal axis is the field amplitude. The black solid line is the theoretical limit. Red squares/blue triangles are for the DCMWP/CFMW. Inset: Optimal chirp rates η for different field amplitudes H_{mw} .

where f_0 is the initial frequency at $t = 0$. The duration of the microwave pulse is $T = \frac{2f_0}{\eta}$ so that the final frequency is $-f_0$.

III. NUMERICAL RESULTS

We first investigate the possibility of reversing the magnetization by a down-chirp microwave pulse (DCMWP). At $t = 0$, $m_z = 1$, and the resonant frequency of the magnetization is $\gamma H_K = 21.0$ GHz. Thus, to make the chirp microwave match the precession of \mathbf{m} as much as possible, we use $f_0 = \gamma H_K = 21.0$ GHz. Figure 2(a) shows the time evolution of m_z under three different microwave fields. The red dashed line shows the reversal by a down-chirp pulse of $f_0 = 21.0$ GHz, $\eta = 67.2$ ns⁻², and $H_{mw} = 0.045$ T. The magnetization reverses quickly with a switching time of 0.6 ns (throughout this paper, the switching time t_s is defined as the time m_z reaches -0.9). As a comparison, the evolution of m_z driven by a microwave of constant frequency (CFMW) 21.0 GHz and the same amplitude 0.045 T is plotted as a black dash-dotted line. The magnetization only precesses around the initial state and does not reverse. To reverse the magnetization by a microwave of constant frequency within the same time (0.6 ns), the amplitude of the field has to be as large as 0.98 T, as shown by the blue solid line, which is unrealistic in practice. Therefore, DCMWP of small amplitude can induce subnanosecond magnetization reversal, showing a significant advantage in comparison with conventional constant-frequency microwave-driven schemes [23,28]. We then investigate how the switching time depends on the chirp rate η and the microwave field amplitude H_{mw} . According to the physical picture discussed in Sec. II, because the changing rate of the frequency should match the magnetization reversal, the duration of the pulse should be close to the switching time. Figure 2(b) shows the η dependence of the switching time t_s for different H_{mw} . The length of the pulse is plotted with a green solid line for comparison. For each H_{mw} , there exists a finite η window in which magnetization reversal occurs. Inside the window, the reversal time depends on η nonmonotonically due to the highly nonlinear magnetization reversal process. However, the reversal times oscillate near the right edge of the window (short pulses). This result justifies

our physical picture that the pulse length is close to the magnetization reversal time. One can also see that the reversal times are not sensitive to η and H_{mw} in the central region of the window. This means a great flexibility in choosing η and H_{mw} as well as the initial frequency, an additional advantageous property in applications. With $\eta = 63.0$ ns⁻² and $H_{mw} = 0.045$ T, the initial frequency can be chosen in a wide range from 20.5 to 39 GHz, with a corresponding reversal time varying from 0.6 to 2 ns.

To have a better sense of how good our strategy is, we compare the optimal reversal time of DCMWP of $f_0 = 21$ GHz and $H_{mw} = 0.045$ – 0.92 T (red squares) with the theoretical limit [20] of the same field amplitude (black solid line) in Fig. 2(c). The corresponding chirp rates for fastest reversal are shown in the inset. The reversal time of CFMW of $f = 21$ GHz is also shown (blue triangles). Below 0.6 T, only DCMWP can switch the magnetization, with a subnanosecond reversal time that is only a little longer than the theoretical limit. For a field amplitude larger than 0.6 T, the constant-frequency microwave is also able to switch the magnetization, but the reversal time is much longer.

In order to have a better physical understanding of the fast switching under DCMWP, we look at the magnetization process in more detail. The red solid line in Fig. 3(a) shows the magnetization reversal process driven by a down-chirp pulse of $f_0 = 21$ GHz, $H_{mw} = 0.045$ T, and $\eta = 67.2$ ns⁻² [which is the same as the parameters used in Fig. 1(a)]. Figure 3(c) shows the trajectory of magnetization reversal. Before (after) the spin passes the equator, it rotates in a counterclockwise (clockwise) direction, as we discussed before. As a comparison, we turn off the field at the moment when \mathbf{m} just passes the equator, so that the energy is purely dissipated by Gilbert damping afterwards, i.e., the first term on the right-hand side of Eq. (3). The black line in Fig. 3(a) shows the magnetization reversal in the case where the chirp field is turned off at the moment when $m_z = -0.004$. It is clear that the second half of the reversal process (from the equator $m_z = 0$ to reversed state $m_z \leq -0.9$) is much slower. Figure 3(b) shows the corresponding trajectory. Obviously, after passing the equator, the magnetization undergoes a high spinning motion and the polar angle goes to the south

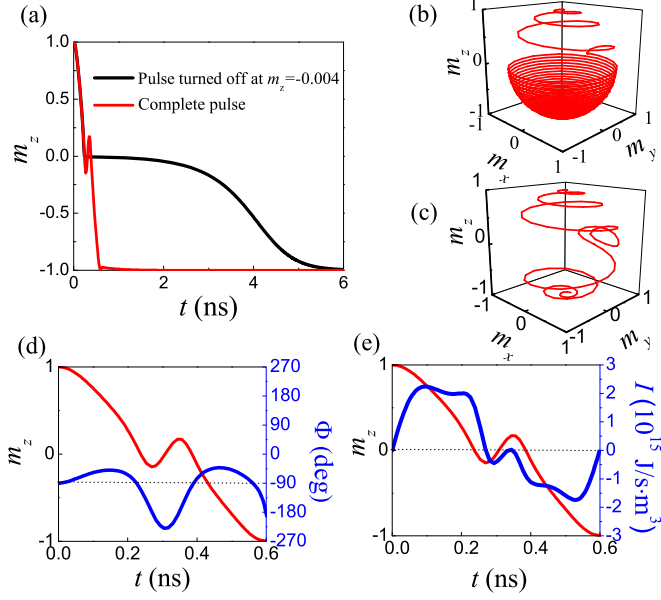


FIG. 3. (a) Magnetization reversal driven by a down-chirp microwave field pulse of $f_0 = 21$ GHz, $H_{mw} = 0.045$ T, and $\eta = 67.2$ ns $^{-2}$. The red line is for a complete pulse. The black line shows magnetization reversal if the pulse is turned off at $m_z = -0.004$. (b) Magnetization trajectory if the field is turned off at the moment when $m_z = -0.004$. (c) Trajectory of magnetization for a complete pulse. (d) Plot of the relative angle Φ against time (blue line) and the time dependence of m_z (red line). (e) Plot of the energy changing rate I of magnetization against time (blue line) and the time dependence of m_z (red line).

pole slowly while the azimuthal angle cycles for many turns. To further justify the physical picture that the down-chirp pulse can trigger stimulated microwave absorptions (emissions) by (from) magnetization before (after) the spin crosses its energy barrier, we look at the angle between the in-plane components of the magnetization and the microwave field. From Eq. (3), the energy changing rate due to the external field is

$$I = -\mathbf{m} \cdot \dot{\mathbf{H}}_{mw} = -H_{mw}\omega(t) \sin \theta(t) \sin \Phi(t), \quad (6)$$

where $\Phi(t)$ is the angle between \mathbf{m}_t (the in-plane component of \mathbf{m}) and \mathbf{H}_{mw} . The blue line in Fig. 3(d) is $\Phi(t)$, and the blue line in Fig. 3(e) is I . Before $t = 0.25$ ns, the magnetization reverses quickly from $m_z = 1$ to the equator, as shown by the red line. At the same time, Φ is around -90° . Because the magnetization precesses counterclockwise ($\omega > 0$), this means \mathbf{H}_{mw} is 0° – 180° behind \mathbf{m}_t . I is positive so that the stimulated microwave absorption occurs. When Φ is -90° , the energy absorption rate reaches the maximum. Also, in Fig. 3(e), the energy changing rate I is positive. Between 0.25 and 0.35 ns, the magnetization oscillates near the equator because of the complicated nonlinear dynamics. After 0.35 ns, the magnetization reverses from the equator to $m_z = -1$. At the same time, Φ is around -90° and the magnetization precesses clockwise ($\omega < 0$). \mathbf{H}_{mw} is 0° to -180° in front of \mathbf{m}_t . I is negative so that the stimulated emission from the particle is triggered. Also, in Fig. 3(e), the energy changing rate I is negative. Thus, the physical picture of fast magnetization

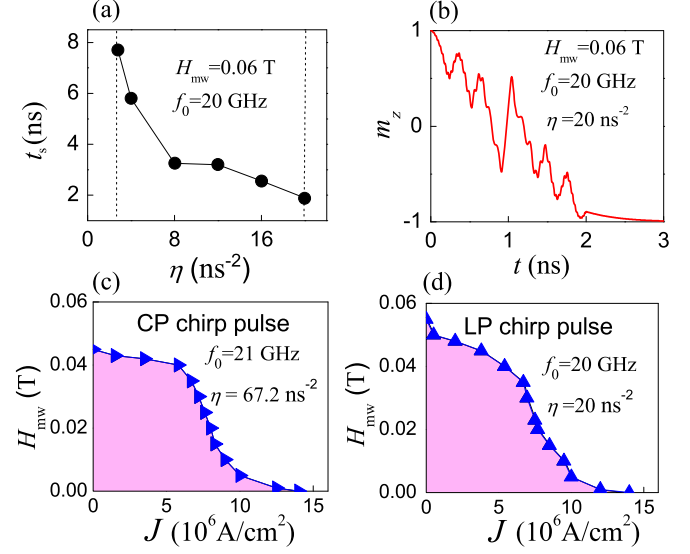


FIG. 4. (a) Dependence of reversal time τ_s on the chirp rate for LP DCMWP of $H_{mw} = 0.06$ T, $f_0 = 20$ GHz. (b) Time evolution of m_z driven by LP DCMWP of $\eta = 20$ ns $^{-2}$, $H_{mw} = 0.06$ T, $f_0 = 20$ GHz. (c), (d) Phase diagram of magnetization reversal in terms of (c) CP and (d) LP DCMWP amplitude H_{mw} and current density J . The pink region means the magnetization does not reverse or the reversal time is longer than 10 ns. The white region means the magnetization reverses within 10 ns.

reversal by a down-chirp microwave pulse is confirmed: For a proper chirp rate and initial frequency, the down-chirp microwave field matches the magnetization precession in a large portion of the reversal process. As a result, before the spin crosses its energy barrier, the microwave field supplies energy to the spin and, after crossing over the energy barrier, the external microwave field triggers a stimulated microwave emission from the spin with a large energy dissipation rate.

In the above studies, we used circularly polarized (CP) microwaves. Many microwave-generation methods, for example, the coplanar waveguide, generate linearly polarized (LP) microwaves. A LP microwave can be decomposed into a linear combination of two CP microwaves with opposite polarizations. So, a down-chirp LP microwave should also be capable of switching a magnetization particle. We numerically demonstrate this capability in Figs. 4(a) and 4(b). Figure 4(a) shows the chirp rate (η) dependence of switching time for a LP microwave of $H_{mw} = 0.06$ T and $f_0 = 20$ GHz. Nanosecond magnetization reversal can be achieved in the window of $\eta = 3.0$ – 20 ns $^{-2}$. Because of the other CP component, the magnetization dynamics becomes more complicated, as shown in Fig. 4(b), which plots the time evolution of m_z for the optimal $\eta = 20$ ns $^{-2}$. The complicated magnetization dynamics also results in a different optimal initial frequency and chirp rate compared to the CP case. The optimal chirp rate is now $\eta = 20$ ns $^{-2}$ for the LP pulse, which is smaller than the CP case, so that the switching time of the LP pulse (2 ns) is also longer than that of the CP pulse.

The obtained microwave magnetic field 0.045 (0.06) T for CP (LP) DCMWP is still too high. To further reduce its value, we can simultaneously apply a dc current. An electric

current is polarized by a fixed layer so that it has a finite polarization along the z direction. Figures 4(c) and 4(d) show the $H_{\text{mw}}-J$ phase diagrams of magnetization reversal for CP and LP chirp microwave pulses, respectively, together with a dc current J . Below (above) the phase boundaries (shown by the blue lines), the switching time is longer (shorter) than 10 ns. The chirp pulses are chosen to be the ones that achieve fast reversal obtained before, i.e., $f_0 = 21$ GHz, $\eta = 67.2$ ns⁻² for the CP microwave and $f_0 = 20$ GHz, $\eta = 20$ ns⁻² for the LP microwave. If we require the switching time to be no longer than 10 ns, for the magnetization reversal by electric current only, the required current density is about 1.4×10^7 A/cm²; for the magnetization reversal by a CP (LP) down-chirp microwave only, the minimal field amplitude is about 0.0445 T (0.06 T). Naturally, in the presence of both chirp wave and electric current, both H_{mw} and J can be smaller than the above values, which provides a large leeway to design practical magnetization reversal strategies according to the technical details.

IV. DISCUSSION AND CONCLUSION

The most challenging part of DCMWP-driven magnetization reversal is the generation of DCMWP with a wide bandwidth and large chirp rates. There are already several possible techniques for chirp-microwave generation, including microwave photonics [37,38]. Recently, it was found that circularly polarized microwaves with time-dependent frequency can be generated by coupling a magnetic nanoparticle to a pair of weak superconducting links [34,39]. The time dependency of the microwave frequency can be controlled by voltage. Another way to generate DCMWP is to use a spin torque oscillator incorporating a field generating layer. By flowing a time varying spin-polarized current through a field generating layer, magnetization oscillation is excited. The oscillating magnetic moment in turn induces microwaves of time-dependent frequency [24,40]. Therefore, the spin torque oscillator acts as a source of DCMWP, with the advantage that it is easy to be integrated with the spin valve to achieve

good locality and scalability. There is already an experimental realization of generating microwaves of time-dependent frequency [41]. The widely used coplanar waveguide can also be used to generate DCMWP. Using two coplanar waveguides, one can generate circularly polarized DCMWP [42] while single coplanar waveguide can be used to generate linearly polarized DCMWP [43]. The DCMWP is characterized by three parameters: the initial frequency f_0 , the chirp rate η , and the field amplitude. According to our simulation and the physical picture of stimulated microwave absorption and emission, one should let f_0 be close to the ferromagnetic resonance (FMR) frequency. The chirp rate η can be tuned from an upper limit $\eta = 2f_0/t_{\text{th}}$, where t_{th} is the theoretical limit [20], because the reversal time t_s is close to the duration of the pulse T , and t_{th} is the lower limit of t_s . The microwave field amplitude should be as large as possible. Our findings provide improvements for the fast magnetization reversal technologies with a clear physical picture, and shine a light on the future development of magnetic data storage and processing devices.

In conclusion, we find a down-chirp microwave pulse can effectively reverse a magnetic nanoparticle. Different from magnetization reversal driven by constant-frequency microwaves through synchronization that requires a strong field, the DCMWP triggers stimulated microwave absorptions (emissions) by (from) the spin before (after) it crosses over the energy barrier, so that the reversal can be fast with a low field by choosing a proper initial frequency and chirp rate. The DCMWP can be used together with a polarized electric current to design more practical reversal strategies.

ACKNOWLEDGMENTS

This work was supported by the National Natural Science Foundation of China (Grant No. 11774296) as well as Hong Kong RGC Grants No. 16300117 and No. 16301816. X.S.W. acknowledges support from UESTC and China Postdoctoral Science Foundation (Grant No. 2017M612932). M.T.I. acknowledges support from a Hong Kong Ph.D. fellowship.

-
- [1] S. Sun, C. B. Murray, D. Weller, L. Folks, and A. Moser, *Science* **287**, 1989 (2000).
 - [2] S. I. Woods, J. R. Kirtley, S. Sun, and R. H. Koch, *Phys. Rev. Lett.* **87**, 137205 (2001).
 - [3] D. Zitoun, M. Respaud, M.-C. Fromen, M. J. Casanove, P. Lecante, C. Amiens, and B. Chaudret, *Phys. Rev. Lett.* **89**, 037203 (2002).
 - [4] *Spin Dynamics in Confined Magnetic Structures I & II*, edited by B. Hillebrands and K. Ounadjela (Springer, Berlin, 2001).
 - [5] S. Mangin, D. Ravelosona, J. A. Katine, M. J. Carey, B. D. Terris, and E. E. Fullerton, *Nat. Mater.* **5**, 210 (2006).
 - [6] A. Hubert and R. Schäfer, *Magnetic Domains* (Springer, Berlin, 1998), Chap. 3.
 - [7] Z. Z. Sun and X. R. Wang, *Phys. Rev. B* **71**, 174430 (2005).
 - [8] J. C. Slonczewski, *J. Magn. Magn. Mater.* **159**, L1 (1996); L. Berger, *Phys. Rev. B* **54**, 9353 (1996).
 - [9] M. Tsoi, A. G. M. Jansen, J. Bass, W.-C. Chiang, M. Seck, V. Tsoi, and P. Wyder, *Phys. Rev. Lett.* **80**, 4281 (1998); J. Sun, *J. Magn. Magn. Mater.* **202**, 157 (1999); Y. B. Bazaliy, B. A. Jones, and S. C. Zhang, *Phys. Rev. B* **57**, R3213(R) (1998).
 - [10] E. B. Myers, D. C. Ralph, J. A. Katine, R. N. Louie, and R. A. Buhrman, *Science* **285**, 867 (1999).
 - [11] A. Brataas, Y. V. Nazarov, and G. E. W. Bauer, *Phys. Rev. Lett.* **84**, 2481 (2000).
 - [12] J. A. Katine, F. J. Albert, R. A. Buhrman, E. B. Myers, and D. C. Ralph, *Phys. Rev. Lett.* **84**, 3149 (2000).
 - [13] X. Waintal, E. B. Myers, P. W. Brouwer, and D. C. Ralph, *Phys. Rev. B* **62**, 12317 (2000).
 - [14] J. Z. Sun, *Phys. Rev. B* **62**, 570 (2000); M. D. Stiles and A. Zangwill, *ibid.* **66**, 014407 (2002); J. Sun, *Nature (London)* **425**, 359 (2003); Z. Li and S. Zhang, *Phys. Rev. B* **68**, 024404 (2003); Y. B. Bazaliy, B. A. Jones, and S. C. Zhang, *ibid.* **69**, 094421 (2004).

- [15] R. H. Koch, J. A. Katine, and J. Z. Sun, *Phys. Rev. Lett.* **92**, 088302 (2004).
- [16] Z. Li and S. Zhang, *Phys. Rev. B* **69**, 134416 (2004); W. Wetzels, G. E. W. Bauer, and O. N. Jouravlev, *Phys. Rev. Lett.* **96**, 127203 (2006).
- [17] J. Grollier, V. Cros, H. Jaffrés, A. Hamzic, J. M. George, G. Faini, J. B. Youssef, H. LeGall, and A. Fert, *Phys. Rev. B* **67**, 174402 (2003).
- [18] H. Morise and S. Nakamura, *Phys. Rev. B* **71**, 014439 (2005); T. Taniguchi and H. Imamura, *ibid.* **78**, 224421 (2008).
- [19] *Nanomagnetism and Spintronics*, edited by T. Shinjo (Elsevier, Amsterdam, 2009), Chap. 3.
- [20] Z. Z. Sun and X. R. Wang, *Phys. Rev. Lett.* **97**, 077205 (2006); X. R. Wang and Z. Z. Sun, *ibid.* **98**, 077201 (2007).
- [21] X. R. Wang, P. Yan, J. Lu, and C. He, *Europhys. Lett.* **84**, 27008 (2008).
- [22] G. Bertotti, C. Serpico, and I. D. Mayergoyz, *Phys. Rev. Lett.* **86**, 724 (2001).
- [23] Z. Z. Sun and X. R. Wang, *Phys. Rev. B* **73**, 092416 (2006); **74**, 132401 (2006).
- [24] J.-G. Zhu and Y. Wang, *IEEE Trans. Magn.* **46**, 751 (2010).
- [25] S. I. Denisov, T. V. Lyutyy, P. Hänggi, and K. N. Trohidou, *Phys. Rev. B* **74**, 104406 (2006).
- [26] S. Okamoto, N. Kikuchi, and O. Kitakami, *Appl. Phys. Lett.* **93**, 102506 (2008).
- [27] T. Tanaka, Y. Otsuka, Y. Furumoto, K. Matsuyama, and Y. Nozaki, *J. Appl. Phys.* **113**, 143908 (2013).
- [28] T. Taniguchi, D. Saida, Y. Nakatani, and H. Kubota, *Phys. Rev. B* **93**, 014430 (2016).
- [29] C. Thirion, W. Wernsdorfer, and D. Mailly, *Nat. Mater.* **2**, 524 (2003).
- [30] K. Rivkin and J. B. Ketterson, *Appl. Phys. Lett.* **89**, 252507 (2006).
- [31] Z. Wang and M. Wu, *J. Appl. Phys.* **105**, 093903 (2009).
- [32] N. Barros, M. Rassam, H. Jirari, and H. Kachkachi, *Phys. Rev. B* **83**, 144418 (2011); N. Barros, H. Rassam, and H. Kachkachi, *ibid.* **88**, 014421 (2013).
- [33] G. Klughertz, P.-A. Hervieux, and G. Manfredi, *J. Phys. D: Appl. Phys.* **47**, 345004 (2014); *Phys. Rev. B* **91**, 104433 (2015).
- [34] L. Cai, D. A. Garanin, and E. M. Chudnovsky, *Phys. Rev. B* **87**, 024418 (2013).
- [35] Y. Zhang, H. Y. Yuan, X. S. Wang, and X. R. Wang, *Phys. Rev. B* **97**, 144416 (2018).
- [36] A. Vansteenkiste, J. Leliaert, M. Dvornik, M. Helsen, F. Garcia-Sanchez, and B. Van Waeyenberge, *AIP Adv.* **4**, 107133 (2014).
- [37] W. Li and J. Yao, *J. Lightwave Technol.* **32**, 3573 (2014).
- [38] S. K. Raghuvanshi, N. K. Srivastava, and A. Srivastava, *Int. J. Electron.* **104**, 1689 (2017).
- [39] L. Cai and E. M. Chudnovsky, *Phys. Rev. B* **82**, 104429 (2010).
- [40] J.-G. Zhu, X. Zhu, and Y. Tang, *IEEE Trans. Magn.* **44**, 125 (2008).
- [41] H. Suto, T. Nagasawa, K. Kudo, K. Mizushima, and R. Sato, *Nanotechnology* **25**, 245501 (2014).
- [42] H. Suto, T. Kanao, T. Nagasawa, K. Mizushima, and R. Sato, *Appl. Phys. Lett.* **110**, 262403 (2017).
- [43] Y. Nozaki, M. Ohta, S. Taharazako, K. Tateishi, S. Yoshimura, and K. Matsuyama, *Appl. Phys. Lett.* **91**, 082510 (2007).